Pharm Res (2011) 28:292–300
DOI 10.1007/s11095-010-0195-6

RESEARCH PAPER

Nanochannel Technology for Constant Delivery of Chemotherapeutics: Beyond Metronomic Administration

Alessandro Grattoni • Haifa Shen • Daniel Fine • Arturas Ziemys • Jaskaran S. Gill • Lee Hudson • Sharath Hosali • Randy Goodall • Xuewu Liu • Mauro Ferrari

Received: 15 March 2010 / Accepted: 11 June 2010 / Published online: 1 July 2010

ABSTRACT

Purpose The purpose of this study is to demonstrate the long-term, controlled, zero-order release of low- and high-molecular weight chemotherapeutics through nanochannel membranes by exploiting the molecule-to-surface interactions presented by nanoconfinement.

Methods Silicon membranes were produced with nanochannels of 5, 13 and 20 nm using standardized industrial microfabrication techniques. The study of the diffusion kinetics of interferonα-2b and leuprolide was performed by employing UV diffusion chambers. The released amount in the sink reservoir was monitored by UV absorbance.

Results Continuous zero-order release was demonstrated for interferonα-2b and leuprolide at release rates of 20 and 100 μg/day, respectively. The release rates exhibited by these membranes were verified to be in ranges suitable for human therapeutic applications.

Conclusions Our membranes potentially represent a viable nanotechnological approach for the controlled administration of chemotherapeutics intended to improve the therapeutic efficacy of treatment and reduce many of the side effects associated with conventional drug administration.

KEY WORDS chemotherapy · controlled release · drug delivery · implants · nanochannel

A. Grattoni · H. Shen · D. Fine · A. Ziemys · J. S. Gill · X. Liu · M. Ferrari
Department of NanoMedicine and Biomedical Engineering (nBME)
The University of Texas Medical School at Houston
Houston, Texas, USA

L. Hudson · S. Hosali · R. Goodall
NanoMedical Systems, Inc.
Austin, Texas, USA

M. Ferrari
Department of Experimental Therapeutics
The University of Texas M.D. Anderson Cancer Center
Houston, Texas, USA

M. Ferrari
Department of Bioengineering, Rice University
Houston, Texas, USA

M. Ferrari (✉)
1825 Pressler St. Suite 537
Houston, Texas 77030, USA
e-mail: mauro.ferrari@uth.tmc.edu

INTRODUCTION

With an estimated 1.48 million reported cases resulting in over 560,000 deaths in 2009, cancer has surpassed heart disease as the leading cause of mortality in the U.S. for individuals 85 years of age and younger (1,2). Despite advances in cancer research, the number of deaths is staggering and growing, while the societal and economic impact of this malignancy continues to be enormous. As an example, the total recurrent annual U.S. market for breast cancer chemotherapies is estimated at $5.9 billion and is expected to continue rising (3).

Nanopharmaceutical compounds such as liposomes (4) and paclitaxel-loaded albumin nanoparticles (5) have been widely used in the clinic (6,7). A large number of novel nanotherapeutics is also involved in ongoing clinical trials (8) and under investigation for the treatment of specific types of cancers (9,10).

Despite the improvement of the therapeutic index of chemotherapeutic compounds achieved through the nanotechnological enhancement of drug formulations, the toxicity associated with drug administration still remains a significant limiting factor (11).

Parallel to the development of targeting strategies has been the investigation of the controlled and metronomic administration of drugs (12). The pharmacodynamics and efficacy of treatments have indeed been demonstrated to be related to the frequency (13), time (14,15) and duration of drug administration. For example, it was shown that the sustained controlled administration of chemotherapeutics for several hours was needed for the drugs to be effective against lymphoma cells (16).

Substantial resources have thus been focused on the development of implantable technologies for the localized controlled administration of drug at therapeutic levels (17–21). Implantable polymeric systems have been developed utilizing release strategies based on both degradation and encapsulation (22). In general, however, polymeric systems lack precise release control, which may represent an obstacle for their adoption to chemotherapy (23). Osmotic pumps (22,24), including the DUROS® developed by the ALZA Corporation, were originally applied to control the release of leuprolide. The device, loaded with 150 µl of a DMSO-based leuprolide solution, showed near-constant release for a year both *in vitro* and in *in vivo* in canines and humans (25). While osmotic pumps have been successfully demonstrated, the requirement of moving components could generate device instabilities, which might lead to therapeutic ineffectiveness or dangerous drug leakage. Other approaches to implantable drug delivery have been investigated by Santini *et al.* (26,27). A microelectromechanical system (MEMS) was developed capable of the pulsatile release of drug molecules from a chip hosting an array of micro-reservoirs capped by gold membranes. The device could selectively open single reservoirs through an applied electrical potential, causing the electrochemical dissolution of the gold membrane. This device was adapted for leuprolide release by MicroCHIPS, Inc. and demonstrated a pulsatile release of leuprolide in a canine model for 6 months (28). Although pulsatile release may be effective for several therapeutic regimes, this system resembles a multiple injection strategy as opposed to continuous drug administration.

Studies have highlighted the efficacy of metronomic strategies for the treatment of various forms of cancer (29,30). The efficacy of such approach as compared to the conventional practice is related to the increased frequency of drug administration at non-toxic doses. In this context, a sustained and continuous administration of therapeutics represents an extreme form of metronomic delivery. As such, nanochannels represent a possibility for a stable therapeutic delivery platform capable of constant, controllable release in a diffusive fashion. Our group was the first to develop silicon nanochannel membranes for biomedical applications (31,32). We proved that when the size of the fluidic channels shrinks to the size of the diffusing molecules, the spatial confinement associated with analyte-to-wall interactions causes a constrained and saturated diffusion. By tailoring the nanochannel size and surface properties, we demonstrated the zero-order release of large biological molecules such as bovine serum albumin (BSA), interferon (INFα-2b) and lysozyme in 13 and 20 nm nanochannels for a period of over 4 weeks (33,34). Furthermore, the membrane materials were shown to be biocompatible (20,35), and implants based on a previous nanochannel membrane architecture demonstrated sustained stable release for 6 months *in vivo*, unaffected by tissue encapsulation (36). Although the results were encouraging, the mechanical stability of the early chip designs was limited. Moreover, manufacturing limitations at that time prevented the investigation of constrained release in channels below 7–10 nm.

In this manuscript, a novel high throughput nanochannel delivery system (nDS) with enhanced mechanical stability is presented. The nDS membranes used in this investigation have nanochannel sizes of 5, 13, or 20 nm, although nanochannels down to 2 nm have been fabricated. These membranes are employed for the *in vitro* constant release of both large and small chemotherapeutic molecules, in this case INFα-2b and leuprolide, at therapeutic levels, a capability which had yet to be reported for low molecular weight pharmaceuticals. INFα-2b is an important immunomodulatory cytokine used alone or in concert with other chemotherapic drugs for the treatment of malignant melanoma (37,38), hairy cell leukemia (39), and giant cell tumor (40). Leuprolide is prescribed for the treatment of prostate cancer (41) (9% of the total cancer deaths in men (1)), ovarian cancer (42) or in chemotherapic cocktails for breast cancer (43), which accounted for 15% of the fatalities among all cancer types in women in 2009.

MATERIALS AND METHODS

Membrane Description

The nanochannel membrane is composed of a silicon substrate and a capping layer. Fig. 1 shows a 3D schematic of the membrane. The silicon substrate presents a mesh structure that provides the mechanical strength of the membrane. The mesh is composed of 50-µm-thick walls separating a regular pattern of 161 square inlet macrochannels (200×200 µm). Inlet microchannels 30 µm in length run through the silicon layer at the bottom of the macrochannels. Outlet microchannels run through a thin capping layer perpendicular to the outer surface. The nanochannels exist in the area between the silicon surface and capping layer, parallel to the chip surface, connecting the inlets to the outlets.

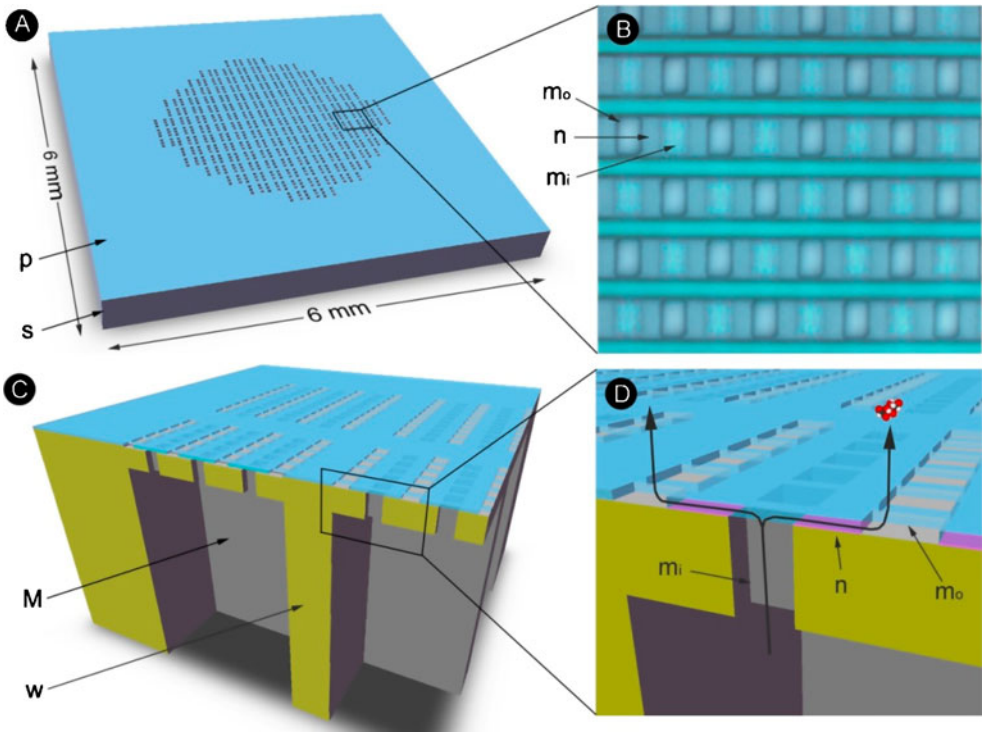

Fig. 1 Schematics (**A**, **C**, **D**) and microscopy image (**B**) of the nanochannel silicon membrane. **A** 3D image of the entire membrane presenting the silicon substrate *s* and the capping layer *p*. **B** optical microscopy image of the membrane surface where m_o, m_i and *n* are the outlet and inlet microchannel and nanochannel, respectively. **C** schematic of the inner membrane structure presenting a mesh of supporting walls *w* and macrochannels *M*. **D** membrane microstructure and the diffusion path of molecules across the membrane. The nanochannels *n* are highlighted in violet.

Membrane Fabrication

The membranes investigated in this study were fabricated using standardized industrial processes at a commercial foundry. A Silicon-on-Insulator (SOI) wafer of diameter 200 mm, with a device layer of 30 μm, a handle layer of 700 μm, and a buried oxide of about 1 μm is used as the substrate. Fabrication of nDS nanofluidic membranes begins with the deposition of a sacrificial layer of a specific thickness. This layer is removed at the end of the process to form the nanochannels. This sacrificial layer is capped with a thin layer of silicon nitride. Rectangular microchannels are dry etched into the silicon nitride, the underlying sacrificial material and through the 30 μm device layer stopping on the buried oxide below. These microchannels are plugged and planarized, and this surface is then patterned to define lines of nanochannels and etched to remove all silicon nitride and the sacrificial material outside of these lines. A thick layer of silicon nitride is then deposited, and outlet microchannels are then patterned on this surface along the lines. The outlet microchannels are etched deep enough to land in the silicon substrate, thus exposing the openings into the nanochannels. The nanochannel arrays are clustered into 161 blocks, each approximately 200 μm×200 μm with a space of 50 μm between them. The wafer is then turned over, and the 161 block regions are patterned with an oxide hard mask. Using a deep silicon etcher, these regions are fully etched out down through the handle silicon, stopping at the buried oxide. The buried oxide is etched away, exposing the bottom of the inlets. The sacrificial materials in the inlets and the nanochannels are then removed with wet-etches, forming a contiguous inlet➔nanochannel➔outlet pathway. nDS chips with nanochannels ranging in size from a few nanometers up to tens of nanometers, with nanochannel densities up to 100,000/mm^2, have been fabricated in quantity.

Experimental Setup

To perform the drug release tests an experimental device was developed. The device is composed of two stainless steel SS316L bodies which house the drug and the sink reservoirs separated by the nanochannel membrane. The membrane is sealed between the metal bodies through two silicone rubber O-rings (Apple Rubber, Lancaster, NY, USA). The drug solution reservoir presents a volume of 150 μl, which is capped through a silicone rubber cap (Mocap, Inc., St. Louis, MO). A 4.45 ml sink reservoir is obtained by bonding the lower metal body to a UV macrocuvette (BrandTech Scientific, Inc. Essex, CT) through an UV-curing epoxy resin (OG116-31, Epoxy Technologies, Billerica, MA). A detailed description of the testing device is presented elsewhere (Grattoni A., Gill J. *et al.* Novel device for nanoscale diffusivity measurements. Anal. Chem. Submitted, (2010)). Fig. 2 shows a schematic of the experimental setup.

Prior to each test, the device's parts were accurately cleaned and autoclaved for 20 min at 121 C. New UV

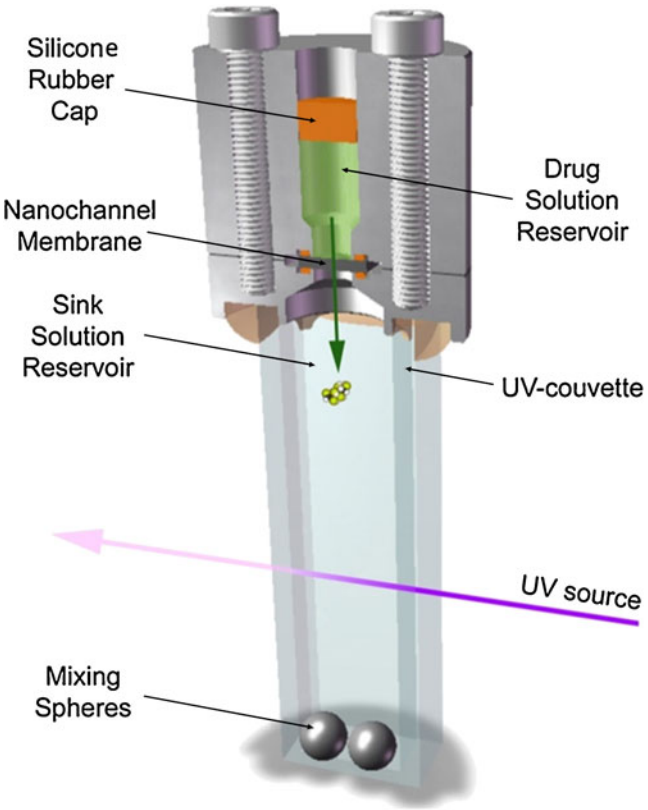

Fig. 2 Testing device parts and assembled device.

cuvettes were used for each experiment. After loading the sink reservoir with phosphate-buffered saline (PBS) (Gibco), the wet membrane was clamped between the reservoirs. Leuprolide (Bachem Americas Inc., Torrance, CA) and INFα-2b (Cell Sciences, Inc., Canton, MA) solutions were prepared in PBS at the concentration 5 mg/ml and 1 mg/ml, respectively. One-hundred-fifty μl of solution was then loaded in the drug solution reservoir. The reservoir was finally capped through a silicone rubber plug pierced by a venting needle. The needle allowed for the complete removal of air and prevented an increase of the pressure within the chamber during the insertion of the plug. The plug was able to self-seal after extraction of the venting needle. The leuprolide release test was performed with continuous magnetic stirring of the sink solution. In the case of INFα-2b, the testing devices were constantly rotated (8 rpm), causing two 5.5-mm stainless steel spheres (SS 316 L) to mix the sink solution by continuous displacement of the fluid. The effectiveness of the mixing procedure was verified by comparing the UV-absorption of the samples before and after vigorous vortexing of the sink solution. No differences were observed in the measurements, demonstrating the homogeneity of the concentration of the solutions achieved through the use of mixing spheres. The tests were carried out at 23±0.2°C over a period of 6 days. Leuprolide release experiments were performed in replicates of 3 for 5 and 13 nm nDS, while INFα-2b tests were executed in 4 replicates using 20 nm nDS. Prior to the diffusion experiment, the membranes were selected through gas testing as described elsewhere (44).

Concentration Measurement

To determine the concentration of drug in the sink solution, the UV absorbance was measured by means of an UV spectrophotometer (DU 730 UV/Vis, Beckman Coulter, Inc.). Absorbance peaks were determined and standard curves generated for leuprolide and INFα-2b at wavelengths of 278 and 230 nm, respectively. The absorbance of each device was measured at several time points. To verify the homogeneity of the sink solution, multiple readings were performed for each time point. Only negligible variations within the repeatability limit of the spectrophotometer were observed. The data were normalized by removing the absorbance at time zero, and the concentration was finally calculated through the standard curves.

RESULTS

INF-Results

The cumulative INFα-2b release, standard deviation, and percentage of the released amount are shown in Fig. 3. The graph shows a linear trend of the experimental points up to a release amount of approximately 95%. The correlation coefficient R^2 between the experimental data and the linear fit was calculated equal to be 0.99. A release rate of approximately 29.7±1.5 μg/day was measured.

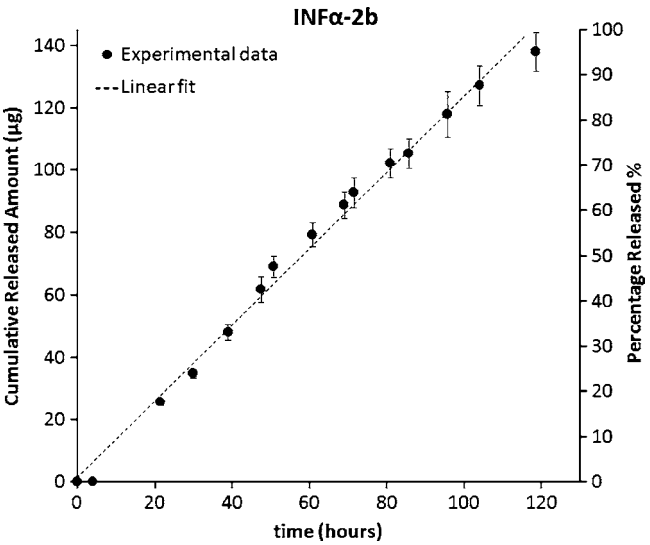

Fig. 3 INFα-2b cumulative release and percentage released.

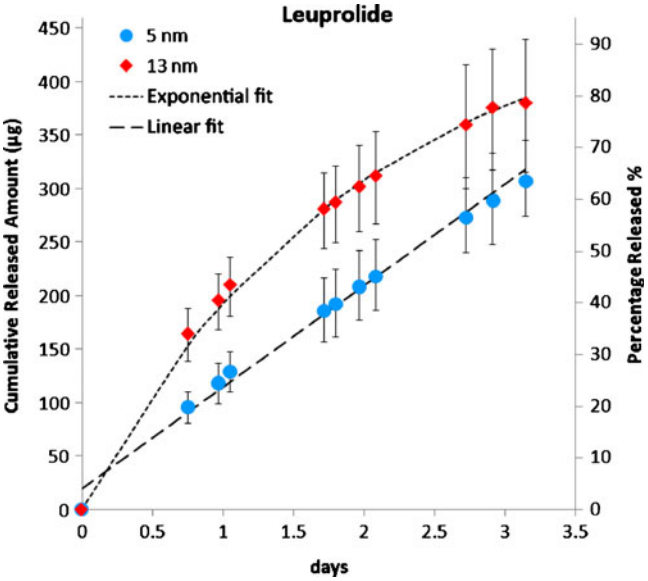

Fig. 4 Leuprolide cumulative release and percentage released throughout 5 and 13 nm nanochannels.

Leuprolide Results

Fig. 4 shows the cumulative release and the percentage of the released amount of leuprolide in 5 and 13 nm nanochannels. The leuprolide released through the 13 nm membrane clearly shows an exponential trend, characteristic of a non-constrained Fickian diffusion. A zero-order release, however, was observed through the 5 nm nanochannels for up to 65% of the total loaded amount. The linear fit of the experimental data presents a correlation coefficient of 0.99. A release rate of approximately 100± 10 µg/day was measured.

The constrained release of INFα-2b and leuprolide is caused by spatial confinement in the nanochannels in which the molecules diffuse. When the channel shrinks to the size of the diffusing molecules, the diffusion becomes two-dimensional and wall-to-molecule interactions dominate the diffusive transport. In particular, leuprolide and INFα-2b tend to adsorb on the native SiO_2 formed on the channel surfaces. This adsorption causes on average a reduction of the effective nanochannel size, which amplifies the molecular confinement. Fig. 5 illustrates the normalized ratio between the size of the molecule and its adsorption exclusion zone to the size of the nanochannel.

The figure clearly shows that the diffusing molecule needs to occupy a significant percentage of the nanochannel height for the release to be constrained. Table I lists the bulk properties of the solutes and the characteristics of their confinement. The table shows that constrained diffusion happens for molecule-to-channel size ratios between 1:3 and 1:5.

DISCUSSION

The conventional bolus administration of drug occurs in periods of time ranging from seconds to minutes. As a consequence, a spike in plasma drug concentration is observed, which generally exceeds the therapeutic range. This temporary drug overdose may emphasize the drug side effects which are generally dose-per-unit time dependent (48). The concentration of the drug in the plasma then slowly decreases, first transitioning to the therapeutic range for a limited period of time and then subsequently falling below the efficacy limit and thus

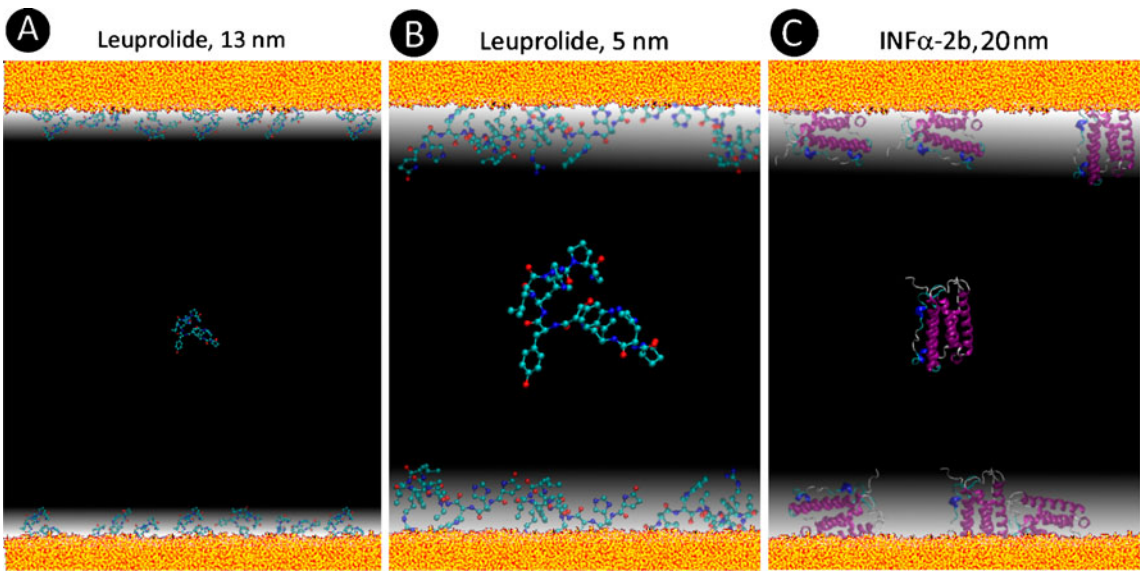

Fig. 5 Schematic representation of leuprolide in 13 and 5 nm (**A** and **B**). Representation of INFα-2b in 20 nm (**C**).

Table I Bulk Properties of Solutes and Confinement Characteristics

Solute	d, nm	d_{min}, nm	q_{net}, e	Mw, kDa	D_B, cm^2/s	nCh, nm	Ratio	$Ratio_{mod}$
LEUP[a]	1.4	1.0	+1	1.2	0.32	5	1:4	1:3
INF α-2b	3.2	3.0	−2	19	0.07	20	1:7	1:5

d – effective size as 2*Rg (radius of gyration) as calculated from the molecular structure; d_{min} – lowest dimension of the molecule; q_{net} – net formal charge of the molecule at pH 7; Mw – molecular mass; D_B – bulk diffusion coefficient at infinite dilution as a multiple of 10^{-5}; nCh – nanochannel height; Ratio – molecule to nanochannel size ratio; $Ratio_{mod}$ – predicted molecule to nanochannel size ratio after including surface adsorption effects

[a] Leuprolide diffusion coefficient is represented by the average of BPTI (Mw = 6.5 kDa 0.15×10^{-5}) (45) and tetrapeptide (0.5×10^{-5}) (46). Interferon diffusion coefficient (47)

requiring a following administration. Alternative to the bolus administration is slow intravenous or intra-arterial infusion, commonly adopted for the administration of chemotherapeutics. The slow infusion allows the plasma drug concentration to reach the therapeutic range and be maintained for a period of time ranging from hours to days. However, this alternative presents the patient with the inconvenience of long visits to the clinic or the discomfort of carrying a catheter infusion device. The ability to control the release rate of drug molecules by tailoring the size and properties of nanochannels presents interesting prospects for the development of new strategies for the administration of chemotherapeutics from implantable devices. The nDS should allow for sustained drug delivery within the therapeutic range while avoiding multiple periodic administrations, reducing the overdosing and side effects associated with conventional practice (generally oral or intravenous), and eliminating the need for a catheter. Improvements in patient compliance and quality of life could also be realized as patients would not be subject to frequent clinic visits for their therapies (49,50). Furthermore, the constant administration of a cocktail of drugs can be achieved through a multi-reservoir nDS implant. A representation of the release profiles of a delivered drug and its concentration in the plasma is plotted *versus* time in Fig. 6 for a conventional intravenous bolus administration, for a slow infusion delivery, and from our zero-order release implant.

The zero-order release from the implant allows for a sustained and time-invariant concentration of drug in the plasma within the therapeutic range once the drug release has equilibrated the kinetics of drug metabolism and body elimination. For instance, here we demonstrate a release rate equal to 100 μg/day for over 3 days for leuprolide, approximating the daily dose administered for prostate cancer patients. This release rate could be sustained for over 6 months from a reservoir presenting a volume of 1 cm^3 and loaded with a leuprolide solution at a concentration of 20 mg/ml. By sustaining the drug concentration in the plasma within the therapeutic range, an increase in the therapeutic index of the treatment may also be possible (48). The implantable zero-order release approach may also reduce the cost of treatment by allowing for a smaller integral amount of drug to be used as compared to conventional strategies (51), especially when considering the possibility of the diminished complexity of the regulatory approval pathway when used in conjunction

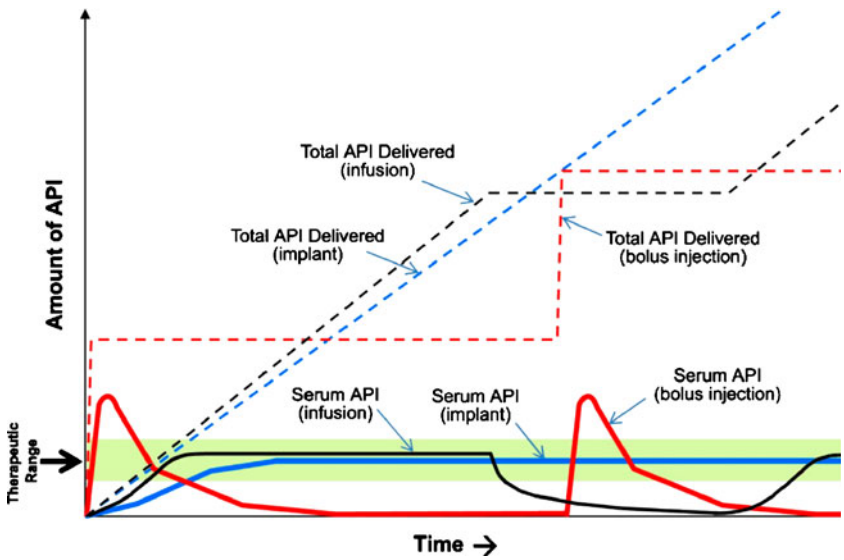

Fig. 6 Profiles of drug delivered and drug concentration in the plasma through bolus injection, infusion, or zero-order release implant.

with already approved therapies. Further cost reductions could be realized by subcutaneous device implantation through a lowered risk of infection when compared to repeated injections or the catheterization required for infusion (48). These savings could offset the cost of the implants which are produced using conventional and well-established manufacturing techniques.

Our nDS has the potential to provide benefit in a broad array of applications in cancer treatment. A local controlled delivery of INFα-2b can be useful in the control of unresectable lesions that are usually accompanied with severe pain (37), in addition to the reduction of the toxicity associated with its systemic administration.

In a recent study, Shah *et al.* showed that the magnitude and duration of drug inhibition were important parameters of tumor cell cytotoxicity when kinase-specific inhibitors were applied to treat lymphoma (16). They found that complete inhibition of the Bcr-Abl kinase activity for at least 8 h was needed before tumor cells committed to cell apoptosis. Neuroendocrine carcinomas have a very low proliferative activity. Conventional chemotherapy is not recommended in the clinic. However, as demonstrated in other studies (52), the low-dose frequent administration of 5-fluorouracil could provide an alternative choice for the treatment of this type of malignancy. A long-term constant drug release could also be effective in the prevention of tumor angiogenesis. It has been shown that low-dose metronomic chemotherapy using trofosfamide did not alter serum VEGF levels while significantly reducing the mobilization of endothelial progenitor cells into the blood of cancer patients. In contrast, conventional dose-dense chemotherapy not only doubled serum VEGF concentrations, but also sharply increased circulating endothelial progenitor cells. Complete inhibition of drug targets over appropriate periods of time might be applicable to most, if not all, drugs for cancer treatment. More in general, the nDS system offers the benefit of extending the duration of drug treatment while keeping a constant drug concentration through controlled release, a feature especially beneficial to drugs with a very short half-life.

The nDS approach may also play an important role in cancer chemoprevention. As an example, about 8% of breast cancer cases are hereditary, and approximately half of these are associated with germline mutations of the breast tumor suppressor gene BRCA1 (53). Women with an inherited BRCA1 or BRCA2 mutation have up to an 80% chance of developing breast cancer during their lifetime. Breast cancer growth is highly dependent on estrogen, and thus inhibition of estrogen is highly effective for the prevention of breast tumor development. The constant local release of an aromatase inhibitor such as letrozole could potentially be effective in the prevention of breast cancer in women at high risk.

CONCLUSIONS

In this work, a novel silicon nanochannel delivery system (nDS) was developed for the zero-order, sustained delivery of chemotherapeutics from implants. The device demonstrated the sustained, controlled release of leuprolide and INFα-2b within the therapeutic range for human applications. By tuning the size and the surface properties of the nanochannels, the nDS technology allowed for the zero-order release of low- and high-molecular-weight molecules. The nDS represents a viable nanotechnological approach for the controlled administration of chemotherapeutics as a potential strategy for the improvement of the therapeutic efficacy of treatment, the reduction of side effects associated with the conventional administration of drugs, and ultimately, the improvement of patient quality of life.

ACKNOWLEDGEMENTS

The authors are grateful to Erika Zabre for her support in the experimental analysis and in the editing of the manuscript. This project has been supported with federal funds from NASA (NNJ06HE06A and NNX08AW91G), Department of Defense (DODW81XWH-09-1-0212), as well as funds from State of Texas Emerging Technology Fund, NanoMedical Systems (NMS), and Alliance of NanoHealth (ANH). The authors acknowledge the Texas Advanced Computing Center (TACC) at the University of Texas at Austin for providing HPC resources that have contributed to the research results reported within this paper.

DISCLOSURE

Grattoni A, Fine D, Liu X and Ferrari M hereby disclose a personal financial interest in NanoMedical Systems, Inc.

REFERENCES

1. American Cancer Society. Cancer facts & figures 2009. Atlanta: American Cancer Society; 2009.
2. Jemal A, Siegel R, Ward E, Hao Y, Xu J, Murray T, *et al.* Cancer statistics, 2008. CA Cancer J Clin. 2008;58:71–96.
3. World Breast Cancer Therapeutics Markets. Frost and Sullivan; 2005.
4. Lyass O, Uziely B, Ben-Yosef R, Tzemach D, Heshing NI, Lotem M, *et al.* Correlation of toxicity with pharmacokinetics of pegylated liposomal doxorubicin (Doxil) in metastatic breast carcinoma. Cancer 2000;89:1037–47.
5. Sparreboom A, Scripture CD, Trieu V, Williams PJ, De T, Yang A, *et al.* Comparative preclinical and clinical pharmacokinetics of a cremophor-free, nanoparticle albumin-bound paclitaxel (ABI-007) and paclitaxel formulated in cremophor (Taxol). Clin Cancer Res. 2005;11:4136–43.
6. Farokhzad OC, Langer R. Impact of nanotechnology on drug delivery. ACS Nano. 2009;3:16–20.
7. Ferrari M. Cancer nanotechnology: opportunities and challenges. Nat Rev Cancer. 2005;5:161–71.

8. Carmo VAS, Ferrari CS, Reis ECO, Ramaldes GA, Pereira MA, De Oliveira MC, *et al.* Biodistribution study and identification of inflammation sites using 99mTc-labelled stealth pH-sensitive liposomes. Nucl Med Commun. 2008;29:33–8.
9. Ferrari M. Frontiers in cancer nanomedicine: directing mass transport through biological barriers. Trends Biotechnol. 2010; 28:181–8.
10. Zhang L, Gu FX, Chan JM, Wang AZ, Langer RS, Farokhzad OC. Nanoparticles in medicine: therapeutic applications and developments. Clin Pharmacol Ther. 2008;83:761–9.
11. Baselt RC. Disposition of toxic drugs and chemicals in man. Biomedical Publications; 2008.
12. Kerbel RS, Klement G, Pritchard KI, Kamen B. Continuous low-dose anti-angiogenic/metronomic chemotherapy: from the research laboratory into the oncology clinic. Ann Oncol. 2002;13:12.
13. Kerbel RS, Kamen BA. The anti-angiogenic basis of metronomic chemotherapy. Nat Rev Cancer. 2004;4:423–36.
14. Hrushesky W. Circadian timing of cancer chemotherapy. Science 1985;228:73–5.
15. Smolensky MH, Peppas NA. Chronobiology, drug delivery, and chronotherapeutics. Adv Drug Deliv Rev. 2007;59:828–51.
16. Shah NP, Kasap C, Weier C, Balbas M, Nicoll JM, Bleickardt E, *et al.* Transient potent BCR-ABL inhibition is sufficient to commit chronic myeloid leukemia cells irreversibly to apoptosis. Cancer Cell. 2008;14:485–93.
17. Wagner V, Dullaart A, Bock A, Zweck A. The emerging nanomedicine landscape. Nat Biotechnol. 2006;24:1211–7.
18. Zafar Razzacki S, Thwar PK, Yang M, Ugaz VM, Burns MA. Integrated microsystems for controlled drug delivery. Adv Drug Deliv Rev. 2004;56:185–98.
19. Nuxoll EE, Siegel RA. BioMEMS devices for drug delivery. IEEE Eng Med Biol Mag. 2009;28:31–9.
20. Voskerician G, Shive MS, Shawgo RS, Recum HV, Anderson JM, Cima MJ, *et al.* Biocompatibility and biofouling of MEMS drug delivery devices. Biomaterials 2003;24:1959–67.
21. Ziaie B, Baldi A, Lei M, Gu Y, Siegel RA. Hard and soft micromachining for BioMEMS: review of techniques and examples of applications in microfluidics and drug delivery. Adv Drug Deliv Rev. 2004;56:145–72.
22. Dash AK, Cudworth II GC. Therapeutic applications of implantable drug delivery systems. J Pharmacol Toxicol Meth. 1998;40:1–12.
23. Staples M, Daniel K, Cima M, Langer R. Application of micro- and nano-electromechanical devices to drug delivery. Pharm Res. 2006;23:847–63.
24. Langer R. New methods of drug delivery. Science 1990; 249:1527–33.
25. Wright JC, Tao Leonard S, Stevenson CL, Beck JC, Chen G, Jao RM, *et al.* An *in vivo/in vitro* comparison with a leuprolide osmotic implant for the treatment of prostate cancer. J Control Release. 2001;75:1–10.
26. Santini Jr JT, Richards AC, Scheidt R, Cima MJ, Langer R. Microchips as controlled drug-delivery devices. Angew Chem Int Ed. 2000;39:2396–407.
27. Santini JT, Cima MJ, Langer R. A controlled-release microchip. Nature 1999;397:335–8.
28. Prescott JH, Lipka S, Baldwin S, Sheppard NF, Maloney JM, Coppeta J, *et al.* Chronic, programmed polypeptide delivery from an implanted, multireservoir microchip device. Nat Biotechnol. 2006;24:437–8.
29. Man S, Bocci G, Francia G, Green SK, Jothy S, Hanahan D, *et al.* Antitumor effects in mice of low-dose (Metronomic) cyclophosphamide administered continuously through the drinking water. Cancer Res. 2002;62:2731–5.
30. Hanahan D, Bergers G, Bergsland E. Less is more, regularly: metronomic dosing of cytotoxic drugs can target tumor angiogenesis in mice. J Clin Invest. 2000;105:1045–7.
31. Chu WH, Ferrari M. In: Microrobotics and micromechanical systems, vol. 2593; SPIE: Philadelphia, PA, USA; 1995. p. 9–20.
32. Desai TA, Chu WH, Tu JK, Beattie GM, Hayek A, Ferrari M. Microfabricated immunoisolating biocapsules. Biotechnol Bioeng. 1998;57:118–20.
33. Martin F, Walczak R, Boiarski A, Cohen M, West T, Cosentino C, *et al.* Tailoring width of microfabricated nanochannels to solute size can be used to control diffusion kinetics. J Control Release. 2005;102:123–33.
34. Cosentino C, Amato F, Walczak R, Boiarski A, Ferrari M. Dynamic model of biomolecular diffusion through two-dimensional nanochannels. J Phys Chem B. 2005;109:7358–64.
35. Kasemo B. Biocompatibility of titanium implants: surface science aspects. J Prosthet Dent. 1983;49:832–7.
36. Walczak R, Boiarski A, Cohen M, West T, Melnik K, Shapiro J, *et al.* Long-term biocompatibility of NanoGATE drug delivery implant. NanoBioTechnology 2005;1:35–42.
37. Lesinski GB, Sharma S, Varker KA, Sinha P, Ferrari M, Carson WE. Release of biologically functional interferon-alpha from a nanochannel delivery system. Biomed Microdevices. 2005;7:71–9.
38. Falkson C, Falkson G, Falkson H. Improved results with the addition of interferon alfa-2b to dacarbazine in the treatment of patients with metastatic malignant melanoma. J Clin Oncol. 1991;9:1403–8.
39. Rai KR, Davey F, Peterson B, Schiffer C, Silver RT, Ozer H, *et al.* Recombinant alpha-2b-interferon in therapy of previously untreated hairy cell leukemia: long-term follow-up results of study by Cancer and Leukemia Group B. Leukemia 1995;9:1116–20.
40. Tamayo L, Ortiz DM, Orozco-Covarrubias L, Duran-McKinster C, Mora MA, Avila E, *et al.* Therapeutic efficacy of interferon alfa-2b in infants with life-threatening giant hemangiomas. Arch Dermatol. 1997;133:1567–71.
41. Cersosimo R, Carr D. Prostate cancer: current and evolving strategies. Am J Health Syst Pharm. 1996;53:381–96.
42. Rao G, Miller D. Clinical applications of hormonal therapy in ovarian cancer. Curr Treat Options Oncol. 2005;6:97–102.
43. Harvey HA, Lipton A, Max DT, Pearlman HG, Diaz-Perches R, de la Garza J. Medical castration produced by the GnRH analogue leuprolide to treat metastatic breast cancer. J Clin Oncol. 1985;3:1068–72.
44. Grattoni A, Rosa ED, Ferrati S, Wang Z, Gianesini A, Liu X, *et al.* Analysis of a nanochanneled membrane structure through convective gas flow. J Micromechanics Microengineering. 2009;19:115018.
45. Wills PR, Georgalis Y. Concentration dependence of the diffusion coefficient of a dimerizing protein. Bovine pancreatic trypsin inhibitor. J Phys Chem. 1981;85:3978–84.
46. Fioroni M, Diaz MD, Burger K, Berger S. Solvation phenomena of a tetrapeptide in water/trifluoroethanol and water/ethanol mixtures: a diffusion NMR, intermolecular NOE, and molecular dynamics study. J Am Chem Soc. 2002;124:7737–44.
47. Burke DC. The purification of interferon. Biochem J. 1961;78:556–63.
48. Sharma S, Nijdam AJ, Sinha PM, Walczak RJ, Liu X, Cheng MM, *et al.* Controlled-release microchips. Expert Opin Drug Deliv. 2006;3:379–94.
49. Danckwerts M, Fassihi A. Implantable controlled release drug delivery systems: a review. Drug Dev Ind Pharm. 1991;17:1465.
50. Velez G, Whitcup SM. New developments in sustained release drug delivery for the treatment of intraocular disease. Br J Ophthalmol. 1999;83:1225–9.

51. Narasimhan B, Langer R. Zero-order release of micro- and macromolecules from polymeric devices: the role of the burst effect. J Control Release. 1997;47:13–20.
52. Brizzi M, Berruti A, Ferrero A, Milanesi E, Volante M, Castiglione F, *et al.* Continuous 5-fluorouracil infusion plus long acting octreotide in advanced well-differentiated neuroendocrine carcinomas. A phase II trial of the Piemonte Oncology Network. BMC Cancer. 2009;9:388.
53. John EM, Miron A, Gong G, Phipps AI, Felberg A, Li FP, *et al.* Prevalence of pathogenic BRCA1 mutation carriers in 5 US racial/ethnic groups. JAMA 2007;298:2869–76.